

# Adsorption Behavior of Nonplanar Phthalocyanines: Competition of Different Adsorption Conformations

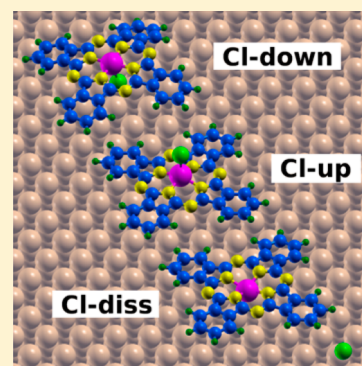
Elisabeth Wruss,<sup>†</sup> Oliver T. Hofmann,<sup>†</sup> David A. Egger,<sup>†,‡</sup> Elisabeth Verwüster,<sup>†</sup> Alexander Gerlach,<sup>§</sup> Frank Schreiber,<sup>§</sup> and Egbert Zojer<sup>\*,†</sup>

<sup>†</sup>Institute of Solid State Physics, NAWI Graz, Graz University of Technology, 8010 Graz, Austria

<sup>§</sup>Institut für Angewandte Physik, Universität Tübingen, 72076 Tübingen, Germany

## S Supporting Information

**ABSTRACT:** Using density functional theory augmented with state-of-the-art van der Waals corrections, we studied the geometric and electronic properties of nonplanar chlorogallium-phthalocyanine GaClPc molecules adsorbed on Cu(111). Comparing these results with published experimental data for adsorption heights, we found indications for breaking of the metal–halogen bond when the molecule is heated during or after the deposition process. Interestingly, the work-function change induced by this dissociated geometry is the same as that computed for an intact adsorbate layer in the “Cl-down” configuration, with both agreeing well with the experimental photoemission data. This is unexpected, as the chemical natures of the adsorbates and the adsorption distances are markedly different in the two cases. The observation is explained as a consequence of Fermi-level pinning due to fractional charge transfer at the interface. Our results show that rationalizing the adsorption configurations on the basis of electronic interface properties alone can be ambiguous and that additional insight from dispersion-corrected DFT simulations is desirable.



## 1. INTRODUCTION

Combining experiments and simulations has become a crucial approach in modern surface science for gaining in-depth atomistic insight into processes at interfaces. It also helps to eliminate certain ambiguities that prevail when interpreting experimental data.<sup>1–3</sup> This is particularly true for X-ray standing wave (XSW) experiments, which allow for the determination of adsorption distances with picometer resolution<sup>4</sup> and are, therefore, of crucial importance for rationalizing interface properties.<sup>5–8</sup> At the same time, such experiments allow for the determination of adsorption geometries only modulo the distance between crystallographic planes parallel to the surface.<sup>9–11</sup> Thus, they can provide two or more possible interpretations for the geometry of the adsorbate. This especially applies to large, nonplanar molecules,<sup>7,12</sup> where unambiguously determining the adsorption height by choosing several nonparallel sets of scattering planes<sup>10</sup> can be difficult. Which of the conceivable adsorption geometries is correct can then be determined using density functional theory (DFT). DFT calculations are also highly useful when investigating the coexistence of different phases and adsorption configurations of molecules on surfaces. They have become particularly powerful over the past few years, as recent advances in the treatment of van der Waals interactions within DFT have hugely increased the reliability of the theoretical results.<sup>13–20</sup> This improvement now allows computations to take a more proactive role in this symbiosis. By means of calculations, it becomes relatively straightforward to test scenarios that usually are not automati-

cally considered, including the dissociation of the adsorbed material.<sup>21</sup>

Such an endeavor lies at the heart of the present work, in which we revisit a previously investigated, very well characterized system: chlorogallium-phthalocyanine (GaClPc) on Cu(111).<sup>12</sup> This system serves as an example of an interface between a nonplanar, polar molecule and a metal, where (i) molecule–metal charge-transfer effects crucially impact the electronic properties and (ii) the determination of the adsorption configuration is far from straightforward. Traditionally, for nonplanar, phthalocyanines (Pcs) the considered adsorption configurations comprise situations in which an intact molecule adsorbs with the molecular backbone parallel to the surface and the central metal atom (or metal–halogen bond) protruding perpendicular to it.<sup>7,20,22–24</sup> Deviating from this common view, we find here that, upon annealing or deposition onto sufficiently heated substrates, a situation with Cl dissociated from the molecule becomes a likely scenario. This process might be more common in Cl-bearing Pcs than hitherto discussed.

## 2. COMPUTATIONAL DETAILS

Using VASP (version 5.3.3),<sup>25</sup> we performed full geometry optimizations, employing the Perdew–Burke–Ernzerhof (PBE) functional<sup>26,27</sup> with projected augmented-wave (PAW)

Received: January 11, 2016

Revised: February 21, 2016

Published: February 29, 2016

potentials<sup>28,29</sup> to treat core–valence interactions (see SI for details). We note that the PBE functional has been shown to cause an incorrect ordering of ligand versus metal-centered states in some metal-Pc<sup>30–32</sup> molecules, which also prevails on noble-metal surfaces.<sup>32,33</sup> For the present interfaces, however, such states do not contribute to the density of states within a few electronvolts of the Fermi energy, as shown in the SI. Thus, we can safely assume that this shortcoming of the PBE functional is not relevant for the present discussion and will not significantly affect the observed charge transfer near the Fermi level. In passing, we note that some of us recently studied the influence of the DFT functional on simulated work functions for the adsorption of various organic molecules on other coinage-metal surfaces.<sup>32,34</sup> The differences in the work functions calculated with either PBE or “conventional” hybrid functionals, such as PBE0 or HSE06, were rather small. We expect that this will be similar for the present system, especially as it is chemically closely related to the systems studied in ref 32. This further justifies the use of the PBE functional.

To account for long-range dispersion forces, the vdW<sup>surf</sup> algorithm<sup>16</sup> specifically tailored to treat adsorption on metallic surfaces was applied. This computationally efficient post-SCF energy-correction scheme combines the vdW-TS dispersion correction approach<sup>14</sup> with Lifshitz–Zaremba–Kohn theory<sup>35,36</sup> to account for nonlocal Coulomb screening at surfaces.<sup>16</sup> It has been shown to yield adsorption distances in excellent agreement with experiment.<sup>16,18,19,32</sup> The van der Waals coefficients  $C_6$ ,  $\alpha$ , and  $R$  for the atoms comprising the GaClPc molecule were taken from ref 14. For Cu, the default settings in VASP 5.3.3 were replaced by the metal-specific parameters from ref 16. A special modification of the VASP code kindly provided by Tomáš Bučko (Comenius University, Bratislava) allowed us to selectively switch off the van der Waals correction between specific atomic species. This was applied here to the interaction between the atoms of the Cu substrate, which is useful because vdW<sup>surf</sup> is not designed to treat van der Waals interactions in the bulk. It also enabled us to use a PBE-optimized lattice constant for Cu (3.637 Å).

For the plane-wave basis, a cutoff energy of 500 eV was set (early steps of geometry optimizations were done with a cutoff energy of 400 eV). The states were occupied according to the Methfessel–Paxton<sup>37</sup> scheme, and a Monkhorst–Pack<sup>38</sup> ( $2 \times 2 \times 1$ )  $k$ -point mesh was applied. To model a surface structure with a metallic substrate, the simulations were performed applying the repeated slab approach with five layers of Cu representing the metal substrate. The periodic replicas of the slab were decoupled by a vacuum region of at least 20 Å containing a self-consistently determined dipole layer compensating for the electrostatic asymmetry of the slab.<sup>39</sup> The geometry optimizations were done using GADGET<sup>40</sup> and VASP. The advanced geometry optimization algorithms implemented in GADGET and the use of a sophisticated model Hessian yield particularly fast convergence properties (see SI for details).<sup>40</sup> During our geometry optimizations, all molecular atoms as well as the top two substrate layers were allowed to relax in all spatial directions until the gradient fell below 0.01 eV/Å. More information on the employed methodology is provided in the SI.

### 3. RESULTS AND DISCUSSION

**3.1. Structure of the Adsorbate Layer.** Based on XSW measurements, ref 12 considers two possible adsorption geometries for GaClPc on Cu(111). These are the so-called

Cl-down configuration, with the Cl atom between the molecular backbone and the surface, and the flipped Cl-up configuration, with Cl pointing away from the surface. The Cl-up interpretation was considered less likely, as it would lead to a strong, energetically unfavorable shortening of the Ga–Cl bond.<sup>12</sup> DFT calculations of the adsorbed molecules placed at the experimental adsorption distances supported the dominance of the Cl-down phase; full geometry optimization including van der Waals (vdW) corrections could not be performed because, at that time, reliable van der Waals corrections were not yet widely available. The assignment of a Cl-down phase was strongly supported by the observation that the calculated work-function shifts upon GaClPc adsorption in the Cl-down configuration agreed almost perfectly with the ultraviolet photoelectron spectroscopy (UPS) data. Notably, the coexistence of Cl-up and Cl-down conformations (or other situations for that matter) was not analyzed in detail. In passing we note that, in ref 12, the UPS results for the annealed GaClPc monolayer were correlated with XSW measurements where the films were deposited at elevated temperature (rather than annealed).<sup>12</sup> It was then assumed that equivalent molecular configurations on the surface were obtained for the two cases, which is, in fact, corroborated by our findings discussed below.

Building on recent advances in available computational methods (vide supra), it is now possible to go beyond the approach outlined above. As a first step, we investigated the above-mentioned Cl-up and Cl-down configurations with one molecule in a rectangular  $\sim 18 \times 18$  Å surface cell (corresponding to approximately 80% coverage; for details, see SI). The resulting fully optimized geometries are shown in Figure 1a,b, and the experimental adsorption heights and the corresponding calculated values are reported in Table 1a,b. As the experiments provide adsorption distances relative to the (hypothetical) unrelaxed topmost metal layer (i.e., relative to the bulk lattice),<sup>9,10</sup> equivalent values are also reported for our simulations (although the surface relaxations of the two topmost metal layers were considered explicitly in the geometry optimization).

For the Cl-up scenario, the molecule stays comparably flat, the Ga–Cl bond is perpendicular to the molecular backbone, and the Ga atom is at a greater distance from the substrate than the molecular plane. We find good agreement between calculated and experimental distances for the C and N atoms. For the metal–halogen group in the center of the molecule, however, the heights disagree by more than 1.0 Å. Moreover, whereas experiments predict that the Ga atom is closer to the substrate than the molecular backbone, simulations clearly position it at a larger distance. The incompatibility between theoretical and experimental results for the Cl-up conformation is, actually, not really surprising, considering that adsorption of GaClPc on Cu(111) in the Cl-up configuration was considered to be inconsistent with the experimental and theoretical data already in ref 12.

In the Cl-down configuration, the GaClPc molecule exhibits an umbrella-like shape that is slightly tilted to the side. Remarkably, also for the Cl-down configuration, the full geometry optimizations performed here yielded adsorption distances clearly deviating from the experimental values: In the simulated structure, the molecule is significantly closer to the surface than one would expect from experiment. This effect is particularly large for the C atoms, where the calculated average C position is by more than 1.2 Å lower than the experimental

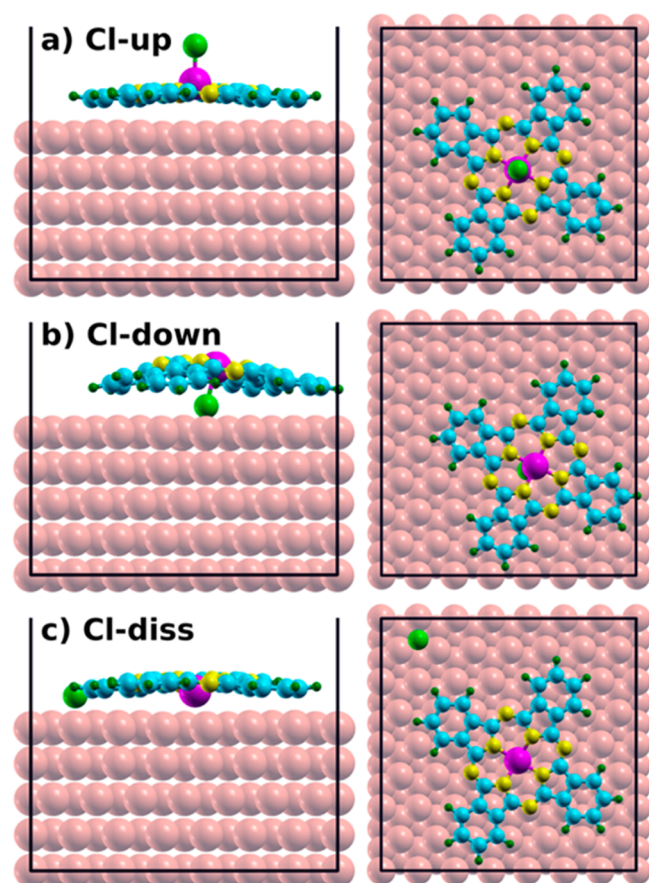


**Figure 1.** Top and side views of the adsorption geometries of a GaClPc molecule on the Cu(111) surface. Adsorption in the (a) Cl-up, (b) Cl-down, and (c) Cl-diss geometries is shown. The molecular atomic species are depicted as follows: C, light blue; H, dark green; N, yellow; Ga, purple; Cl, light green. The unit cell is indicated by solid black lines.

**Table 1. Adsorption Heights (Å) of the Different Atomic Species of the GaClPc Molecule on Cu(111), as Obtained by Experiments (XSW)<sup>12</sup> and Simulations (DFT), for the (a) Cl-up, (b) Cl-down, and (c) Cl-diss Scenarios<sup>a</sup>**

atom	(a) Cl-up		(b) Cl-down		(c) Cl-diss	
	XSW	DFT	XSW	DFT	XSW	DFT
C	2.36(7)	2.45	4.44(7)	3.18	2.36(7)	2.51
N	2.63(3)	2.58	4.71(3)	3.72	2.63(3)	2.68
Ga	2.13(5)	3.14	4.21(5)	3.79	2.13(5)	2.14
Cl	3.96(3)	5.36	1.88(3)	1.51	1.88(3)	1.86

<sup>a</sup>To better suit the different molecular configurations, the XSW results were interpreted differently for the three configurations by adding appropriate numbers of bulk lattice plane spacings [2.08 Å for Cu(111)<sup>12</sup>].<sup>9,10</sup>

value. Also the experimental finding that Ga is positioned below the average C adsorption height cannot be reproduced computationally for the Cl-down structure. To clarify the origin of these deviations, we studied a significant number of variations in unit cell size and starting geometry. They all yielded qualitatively similar deviations from the experimental structure (see SI for details).

The lack of agreement between the measured and calculated adsorption distances implies that other, hitherto-uninvestigated adsorbate structures have to be taken into account. In this

context, an intriguing aforementioned observation is that, in the Cl-up conformation, the geometry of the backbone is already very close to that observed by experiment, with the discrepancy lying “only” in the positions of the central two atoms. This raises the question which modifications in the adsorption configuration would change that situation. In this context, it is interesting that, in several instances, partial and/or full dechlorination of metal-bonded Cl atoms in organic films on coinage-metal substrates has been reported upon adsorption and/or annealing.<sup>21,41,42</sup> Therefore, considering that the Cu surface can promote molecular dissociation,<sup>43,44</sup> another potentially realistic scenario is that the Cl atom is separated from the rest of the molecule.

In the case of GaClPc on Cu(111), it is clear that the Cl atom remains on the surface, as can be inferred from the XSW results and the associated X-ray photoelectron spectroscopy (XPS) characterization.<sup>12</sup> Therefore, we simulated a situation with the GaPc and Cl fragments adsorbing side by side on the Cu(111) surface separated by more than 4 Å to prevent spurious interactions (structure Cl-diss in Figure 1c). In passing we note that, as a test, we also considered a situation in which the Cl atom was removed from the unit cell, mimicking a situation in which the Cl atom has diffused away from the molecule. This simulation yields adsorption distances for the remaining GaPc system that are virtually identical to those in the Cl-diss case.

The geometry of the molecular backbone of the Cl-diss configuration is very similar to that of the Cl-up configuration, adsorbing essentially flat on the surface. A notable exception is the Ga atom, which—in contrast to the Cl-up case—is located below the organic backbone, that is, between the backbone and the substrate (Table 1c). We attribute this difference to the Ga atom no longer being saturated by the bond to the Cl atom, which triggers a stronger interaction with the Cu surface. Overall, the quantitative agreement between the measured and calculated adsorption distances is excellent for both the molecular constituents and the Cl atom. Remaining deviations are in the range of a few hundredths of an angstrom. Only for the C atoms are they somewhat larger (0.15 Å). In this context, it is interesting to note that the calculated C adsorption heights spread over 0.48 Å. This is related to the 4-fold symmetry of the molecule being reduced to a 2-fold symmetry upon adsorption on the 6-fold symmetric-top layer of the substrate. This leads to two of the four molecular branches bending more strongly and, thus, coming significantly closer to the Cu surface (see SI for details). Regarding the Cl adsorption positions, it is worth mentioning that both the measured and calculated adsorption distances are similar to literature values for isolated Cl atoms on Cu(111).<sup>45</sup> The overall excellent agreement between the measured adsorption distances and the calculations for the Cl-diss conformation implies that the dechlorination of at least some of the GaClPc molecules is a realistic scenario, especially upon deposition at elevated temperature (i.e., for the samples used in the XSW experiments in ref 12) or upon annealing of the films (as in the UPS experiments, *vide infra*).

### 3.2. Configuration-Dependent Adsorption Energy.

The possibility of a splitting-off of the Cl atom at the Cu(111) surface is further supported by the relative adsorption energies. These energies were obtained for the different configurations by subtracting the energies of the separately geometry-optimized isolated molecule ( $E_{\text{molecule}}$ , optimized in a converged  $45 \times 45 \times 40 \text{ Å}^3$  unit cell) and the geometry-

optimized metal slab ( $E_{\text{slab}}$ ) from the total energy of the combined system discussed so far ( $E_{\text{system}}$ )

$$E_{\text{ads}} = E_{\text{system}} - E_{\text{molecule}} - E_{\text{slab}} \quad (1)$$

The results are reported in Table 2, together with the corresponding contributions arising from van der Waals

**Table 2. Adsorption Energies ( $E_{\text{ads}}$ ) and van der Waals Contributions ( $E_{\text{ads,vdW}}$ ) per Molecule for GaClPc on the Cu(111) Surface in the (a) Cl-up, (b) Cl-down, and (c) Cl-diss Configurations**

configuration	$E_{\text{ads}}$ (eV)	$E_{\text{ads,vdW}}$ (eV)
(a) Cl-up	-4.72	-6.47 <sup>a</sup>
(b) Cl-down	-2.65	-4.24
(c) Cl-diss	-5.10	-6.47 <sup>a</sup>

<sup>a</sup>Note that the identical values of  $E_{\text{ads,vdW}}$  for Cl-up and Cl-diss are a coincidence.

interactions. The latter strongly contribute to the adsorption energies, which implies that suitable theoretical tools for describing van der Waals interactions are a crucial prerequisite for reliably optimizing the geometries of such systems.<sup>15,16,18,19,32</sup> The significantly lower (i.e., less negative) adsorption energy of Cl-down compared to the two other configurations is a consequence of the much larger adsorption distance of the molecular backbone and, thus, a significantly reduced van der Waals attraction. While Cl-up and Cl-diss lie at very similar adsorption distances, Cl-diss is more strongly bonded to the surface.

At this point, it should be stressed that adsorption energies only point to the thermodynamically most stable configuration, neglecting any kinetic effects. In the present case, it appears likely that a certain activation barrier is associated with the splitting-off of the Cl atoms. As a consequence, depending on the film growth and the annealing conditions, the coexistence of several configurations (Cl-up, Cl-down, Cl-diss) is certainly a viable scenario with a considerable impact on the expected experimental data. This possibility would be consistent with Cl dissociation appearing especially when films are grown on substrates at elevated temperatures (for XSW experiments) or when a sample is annealed (as for the UPS measurements discussed below).<sup>12</sup> It should also be mentioned here that the exact value of the adsorption energy for the Cl-diss scenario depends on the fate of the Cl atom. Although it is known from XSW experiments that the Cl atom remains on the Cu(111) surface, it might adsorb in different positions, such as at step edges, and/or Cl atoms could form islands. Although our simulations do not focus on elucidating the detailed mechanism of the dechlorination reaction, it is worth mentioning that some mechanistic insight can be gained from previous studies on related systems.<sup>21,46</sup>

### 3.3. Adsorption-Induced Work-Function Modification.

The fact that our simulations of geometry and binding energies support a Cl-diss scenario raises an important issue: A strong argument for the prevalence of the Cl-down configuration has been that the computed work-function modification,  $\Delta\Phi$ , for this conformation (-0.55 eV for the Cl-down structure simulated in ref 12) is in excellent agreement with that measured after annealing the sample at 300 °C (-0.60 eV measured by UPS).

This calls for an in-depth investigation of the work-function changes caused by the organic adsorbate layer. Interestingly, the

value of  $\Delta\Phi$  that we computed for the fully relaxed Cl-down conformation ( $\Delta\Phi = -0.58$  eV, cf. Table 3) is essentially the

**Table 3.  $\Delta\Phi$  Values of the Cu(111) Surface upon Adsorption of GaClPc in Different Configurations, Including Contributions Originating from the Molecular Dipole ( $\Delta\Phi_{\text{dip}}$ ) and the Bonding-Induced Dipole ( $\Delta\Phi_{\text{bond}}$ )<sup>a</sup>**

	$\Delta\Phi$ (eV)	$\Delta\Phi_{\text{dip}}$ (eV)	$\Delta\Phi_{\text{bond}}$ (eV)
Cl-up	-0.37	0.23	-0.58
Cl-down	-0.58	-0.26	-0.30
Cl-diss <sup>b</sup>	-0.62	-0.08	-0.53
experimental <sup>12</sup>			
before annealing	-0.34		
after annealing	-0.60		
Cl-down from ref 12	-0.55	-0.30	-0.25

<sup>a</sup>The minimal deviations from eq 2 arise from the asymmetry of the slab due to rearrangements of the top two Cu rows, which were neglected in the derivation of  $\Delta\Phi_{\text{bond}}$ .<sup>b</sup>To avoid effects of spurious charge transfer in the Cl-diss case between the GaPc molecule and the Cl atom, these two fragments were calculated separately (see SI for details).

same as the computational value reported in ref 12 ( $\Delta\Phi = -0.55$  eV, cf. Table 3) despite the very significant differences in adsorbate geometries: Whereas we fully optimized the geometries, in ref 12, fixed adsorption heights determined from experimental values were used. For Cl-down, the latter approach resulted in a molecular backbone that was more than 1.0 Å higher than when the geometry was fully optimized (cf., Table 1). Even more surprisingly, an equivalent value for the work-function change is obtained for the Cl-diss case ( $\Delta\Phi = -0.62$  eV; see Table 3), which is intriguing considering that the highly polar Ga-Cl bond is no longer intact. In passing, we note that, for the situation with Cl removed from the unit cell, we also obtain a value of  $\Delta\Phi = -0.65$  eV, which, as for all other calculated values mentioned so far, would be consistent with the experimental  $\Delta\Phi$  value of -0.60 eV obtained after annealing. The only GaClPc configuration considered in this work that induces a markedly different work-function modification is Cl-up: Its  $\Delta\Phi$  of -0.37 eV is, however, very close to the -0.34 eV measured for GaClPc films grown at 80 °C prior to annealing at 300 °C.<sup>12</sup>

To understand the origin of the very similar work-function modifications induced by the Cl-down and Cl-diss configurations, it is useful to split the total work-function change into two parts: first, the contribution stemming from the dipoles of the molecules that form the adsorbate layer,  $\Delta\Phi_{\text{dip}}$ , and second, the contribution from the charge rearrangements at the surface. The latter cause the so-called bond dipole,  $\Delta\Phi_{\text{bond}}$ .<sup>47,48</sup> For the overall work-function change, one then obtains

$$\Delta\Phi = \Delta\Phi_{\text{dip}} + \Delta\Phi_{\text{bond}} \quad (2)$$

To calculate  $\Delta\Phi_{\text{dip}}$ , the molecules are arranged in a (hypothetical) free-standing monolayer in exactly the geometry they would adopt on the surface.  $\Delta\Phi_{\text{bond}}$  is obtained by solving Poisson's equation using the bonding-induced charge rearrangements as a source term (see SI for details). The values of  $\Delta\Phi_{\text{dip}}$  and  $\Delta\Phi_{\text{bond}}$  for all systems are listed in Table 3.  $\Delta\Phi_{\text{dip}}$  can be understood from the adsorption geometries of the different conformations: When Cl is significantly above the  $\pi$ -backbone, the orientation of the molecular dipole causes a shift in the work function of +0.23 eV. Reversing the dipole

orientation in Cl-down results in a change in sign of the molecule-related work-function modification, and  $\Delta\Phi_{\text{dip}}$  becomes  $-0.26$  eV. For Cl-diss, the Ga–Cl dipole disappears ( $\Delta\Phi_{\text{dip}} = -0.08$  eV). When comparing  $\Delta\Phi_{\text{bond}}$  for Cl-down and Cl-diss, one observes that the smaller  $\Delta\Phi_{\text{dip}}$  value for Cl-diss is accompanied by a larger  $\Delta\Phi_{\text{bond}}$  value, such that, as a net effect, the total work-function modifications become essentially the same. The fundamental reason for this result is rooted in the filling of the molecular states upon adsorption: As shown in Figure 2, where the density of states projected onto the

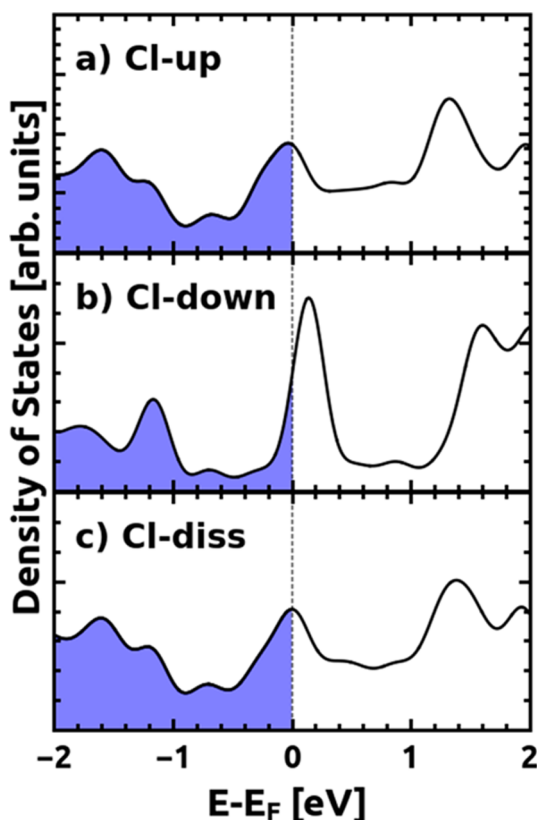


**Figure 2.** PBE-calculated densities of states projected onto the adsorbed GaClPc layer for the (a) Cl-up, (b) Cl-down, and (c) Cl-diss configurations. The energy is aligned to the Fermi energy, which is indicated by a dotted line. The blue region indicates the filled states. The PDOSs were obtained on the basis of fully optimized geometries.

molecular layer (PDOS) is drawn, in all considered cases, a partially filled molecule-derived band at the Fermi energy is observed. That is, the Fermi level cuts through the peak associated with the band derived from the lowest unoccupied molecular orbital (LUMO).

This scenario results in Fermi-level pinning, namely, a situation in which the system work function becomes independent of the work function of the substrate.<sup>34,49–54</sup> Then, it is essentially the energy of the “molecular pinning level” that determines the work function, at least as long as (i) all molecular dipoles are located spatially between the metal substrate and the molecular states at which the Fermi level is pinned<sup>54</sup> and (ii) the packing density is sufficiently high.<sup>55</sup> In such a case,  $\Delta\Phi_{\text{bond}}$  has to compensate for differences in  $\Delta\Phi_{\text{dip}}$ . This is exactly what happens here for Cl-down and Cl-diss. The equality of  $\Delta\Phi$  for Cl-down and Cl-diss thus implies that the characters and energetics of the LUMO-derived bands after adsorption are essentially the same in the two systems, an

assessment that is fully confirmed by calculating the energetic positions of those bands relative to the vacuum energy in the (hypothetical) free-standing molecular monolayers.

The situation is fundamentally different when the molecular dipole is located farther from the substrate than the pinned molecular levels, as is the case for Cl-up. Then, this dipole induces an additional shift in the electrostatic energy beyond the value determined by Fermi-level pinning.<sup>54</sup> Thus, for Cl-up,  $\Delta\Phi_{\text{bond}}$  is essentially the same as the total work-function shift of Cl-down and Cl-diss (i.e., determined by the energy of the level at which the molecular backbone is pinned). In addition, there is a work-function change of  $+0.23$  eV due to the arrangement of the Ga–Cl dipoles above the molecules.

As mentioned before, the obtained work-function change of  $-0.37$  eV for Cl-up is intriguingly close to the largest work-function reduction of  $-0.34$  eV that is measured for GaClPc films deposited at  $80$  °C prior to annealing.<sup>12</sup> This potentially indicates that, in this case, a large portion of the molecules adopt the Cl-up configuration, which is energetically favorable over Cl-down (see Table 2). Although it cannot be excluded that part of the GaClPc molecules arriving in a Cl-down configuration lose their Cl atom right upon adsorption [as reported for FeOEP-Cl on Cu(111)<sup>21</sup>], a more substantial loss of Cl atoms apparently occurs only when the films are deposited at elevated temperatures or when the samples are annealed.

#### 4. CONCLUSIONS

The commonly considered geometric configurations for phthalocyanines (Pcs) with central metal-halide substituents comprise situations with the halide groups pointing either toward or away from the substrate. Here, we suggest a different situation to be the thermodynamically most stable case [at least on the Cu(111) surface], namely, dissociation of the molecule with the Cl atom split off from the Pc backbone. The calculated adsorbate geometry for such a situation is in excellent agreement with previously published X-ray standing wave data for that interface. Interestingly, we find essentially identical work-function changes for a number of cases: (i) the experiments, (ii) previous calculations for GaClPc on Cu(111) in the Cl-down configuration (ref 12) at fixed geometries, (iii) a fully optimized Cl-down geometry, and (iv) the geometry with the Cl atom split off the molecular backbone. This is surprising, given that the calculated adsorption geometries in configurations ii–iv are vastly different. This apparent conundrum is resolved by associating the work-function changes with Fermi-level pinning. A situation in which a significant fraction of the GaClPc molecules dissociate and GaPc and Cl adsorb separately is fully consistent with the available experimental data for situations in which enough energy has been provided to overcome the activation energy barrier for dissociation; depending on the annealing time/film growth temperature, the coexistence of different phases (Cl-up, Cl-down, Cl-diss) is also a viable scenario. The described dissociation effects of halogens might play a crucial role for other interfaces as well, especially those including reactive surfaces such as Cu(111).<sup>21,44</sup> This implies that particular care must be taken during any annealing procedures and that scenarios similar to the one presented here have to be taken into account when one is trying to understand experimental observations.

## ■ ASSOCIATED CONTENT

### Supporting Information

The Supporting Information is available free of charge on the ACS Publications website at DOI: 10.1021/acs.jpcc.6b00312.

Details on PAW potentials, GADGET calculations, unit cells, geometry changes during geometry optimizations, additional test calculations, calculations of charge rearrangements and bond dipoles, discussion of symmetry reduction upon adsorption, and densities of states projected onto the adsorbate layer and separately onto the Ga atoms (PDF)

## ■ AUTHOR INFORMATION

### Corresponding Author

\*E-mail: [egbert.zojer@tugraz.at](mailto:egbert.zojer@tugraz.at).

### Present Address

<sup>‡</sup>D.A.E.: Department of Materials and Interfaces, Weizmann Institute of Science, Rehovoth 76100, Israel.

### Author Contributions

The manuscript was written through contributions of all authors. All authors have given approval to the final version of the manuscript

### Notes

The authors declare no competing financial interest.

## ■ ACKNOWLEDGMENTS

Financial support by the Austrian Science Fund (FWF) P24666-N20, is gratefully acknowledged. Part of the work of D.A.E. was supported by a DOC fellowship from the Austrian Academy of Sciences. We thank Tomáš Bučko (Comenius University, Bratislava) for support with the computational methods. The computational results presented were achieved using the Vienna Scientific Cluster (VSC) and the clusters of the scientific computing department of Graz University of Technology (ZID).

## ■ REFERENCES

- (1) Hauschild, A.; Karki, K.; Cowie, B. C. C.; Rohlfing, M.; Tautz, F. S.; Sokolowski, M. Molecular Distortions and Chemical Bonding of a Large Pi-Conjugated Molecule on a Metal Surface. *Phys. Rev. Lett.* **2005**, *94*, 036106.
- (2) Romaner, L.; Heimel, G.; Brédas, J.-L.; Gerlach, A.; Schreiber, F.; Johnson, R. L.; Zegenhagen, J.; Duhm, S.; Koch, N.; Zojer, E. Impact of Bidirectional Charge Transfer and Molecular Distortions on the Electronic Structure of a Metal-Organic Interface. *Phys. Rev. Lett.* **2007**, *99*, 256801.
- (3) Stadtmüller, B.; Lüftner, D.; Willenbockel, M.; Reinisch, E. M.; Sueyoshi, T.; Koller, G.; Soubatch, S.; Ramsey, M. G.; Puschnig, P.; Tautz, F. S.; Kumpf, C. Unexpected Interplay of Bonding Height and Energy Level Alignment at Heteromolecular Hybrid Interfaces. *Nat. Commun.* **2014**, *5*, 3685.
- (4) Gerlach, A.; Bürker, C.; Hosokai, T.; Schreiber, F. X-ray Standing Wave and Surfaces X-ray Scattering Studies of Molecule–Metal Interfaces. In *The Molecule–Metal Interface*; Koch, N., Ueno, N., Wee, A. T. S., Eds.; John Wiley & Sons: Weinheim, Germany, 2013; Chapter 6.
- (5) Stanzel, J.; Weigand, W.; Kilian, L.; Meyerheim, H. L.; Kumpf, C.; Umbach, E. Chemisorption of NTCDA on Ag(1 1 1): A NIXSW Study Including Non-Dipolar and Electron-Stimulated Effects. *Surf. Sci.* **2004**, *571*, L311–L318.
- (6) Gerlach, A.; Schreiber, F.; Sellner, S.; Dosch, H.; Vartanyants, I. A.; Cowie, B. C. C.; Lee, T.-L.; Zegenhagen, J. Adsorption-Induced Distortion of F16CuPc on Cu(111) and Ag(111): An X-Ray Standing

Wave Study. *Phys. Rev. B: Condens. Matter Mater. Phys.* **2005**, *71*, 205425.

- (7) Stadler, C.; Hansen, S.; Pollinger, F.; Kumpf, C.; Umbach, E.; Lee, T.-L.; Zegenhagen, J. Structural Investigation of the Adsorption of SnPc on Ag(111) Using Normal-Incidence X-Ray Standing Waves. *Phys. Rev. B: Condens. Matter Mater. Phys.* **2006**, *74*, 035404.

- (8) Koch, N.; Gerlach, A.; Duhm, S.; Glowatzki, H.; Heimel, G.; Vollmer, A.; Sakamoto, Y.; Suzuki, T.; Zegenhagen, J.; Rabe, J. P.; et al. Adsorption-Induced Intramolecular Dipole: Correlating Molecular Conformation and Interface Electronic Structure. *J. Am. Chem. Soc.* **2008**, *130*, 7300–7304.

- (9) Zegenhagen, J. Surface Structure Determination with X-Ray Standing Waves. *Surf. Sci. Rep.* **1993**, *18*, 202–271.

- (10) Woodruff, D. P. Surface Structure Determination Using X-Ray Standing Waves. *Rep. Prog. Phys.* **2005**, *68*, 743.

- (11) Gerlach, A.; Schreiber, F. The X-ray Standing Wave Technique. In *Handbook of Spectroscopy*, 2nd ed.; Gauglitz, G., Moore, D. S., Eds.; John Wiley & Sons: Weinheim, Germany, 2014; Chapter 44.

- (12) Gerlach, A.; Hosokai, T.; Duhm, S.; Kera, S.; Hofmann, O. T.; Zojer, E.; Zegenhagen, J.; Schreiber, F. Orientational Ordering of Nonplanar Phthalocyanines on Cu(111): Strength and Orientation of the Electric Dipole Moment. *Phys. Rev. Lett.* **2011**, *106*, 156102.

- (13) Grimme, S. Semiempirical GGA-Type Density Functional Constructed with a Long-Range Dispersion Correction. *J. Comput. Chem.* **2006**, *27*, 1787–1799.

- (14) Tkatchenko, A.; Scheffler, M. Accurate Molecular van der Waals Interactions from Ground-State Electron Density and Free-Atom Reference Data. *Phys. Rev. Lett.* **2009**, *102*, 073005.

- (15) Mercurio, G.; McNellis, E. R.; Martin, I.; Hagen, S.; Leyssner, F.; Soubatch, S.; Meyer, J.; Wolf, M.; Tegeder, P.; Tautz, F. S.; Reuter, K. Structure and Energetics of Azobenzene on Ag(111): Benchmarking Semiempirical Dispersion Correction Approaches. *Phys. Rev. Lett.* **2010**, *104*, 036102.

- (16) Ruiz, V. G.; Liu, W.; Zojer, E.; Scheffler, M.; Tkatchenko, A. Density-Functional Theory with Screened van Der Waals Interactions for the Modeling of Hybrid Inorganic-Organic Systems. *Phys. Rev. Lett.* **2012**, *108*, 146103.

- (17) Klimeš, J.; Michaelides, A. Perspective: Advances and Challenges in Treating van Der Waals Dispersion Forces in Density Functional Theory. *J. Chem. Phys.* **2012**, *137*, 120901.

- (18) Bürker, C.; Ferri, N.; Tkatchenko, A.; Gerlach, A.; Niederhausen, J.; Hosokai, T.; Duhm, S.; Zegenhagen, J.; Koch, N.; Schreiber, F. Exploring the Bonding of Large Hydrocarbons on Noble Metals: Diindoperylene on Cu(111), Ag(111), and Au(111). *Phys. Rev. B: Condens. Matter Mater. Phys.* **2013**, *87*, 165443.

- (19) Egger, D. A.; Ruiz, V. G.; Saidi, W. A.; Bučko, T.; Tkatchenko, A.; Zojer, E. Understanding Structure and Bonding of Multilayered Metal–Organic Nanostructures. *J. Phys. Chem. C* **2013**, *117*, 3055–3061.

- (20) Huang, Y. L.; Chen, W.; Bussolotti, F.; Niu, T. C.; Wee, A. T. S.; Ueno, N.; Kera, S. Impact of Molecule–Dipole Orientation on Energy Level Alignment at the Submolecular Scale. *Phys. Rev. B: Condens. Matter Mater. Phys.* **2013**, *87*, 085205.

- (21) van Vörden, D.; Lange, M.; Schaffert, J.; Cottin, M. C.; Schmuck, M.; Robles, R.; Wende, H.; Bobisch, C. A.; Möller, R. Surface-Induced Dechlorination of FeOEP-Cl on Cu(111). *Chem-PhysChem* **2013**, *14*, 3472–3475.

- (22) Duncan, D. A.; Unterberger, W.; Hogan, K. A.; Lerotholi, T. J.; Lamont, C. L. A.; Woodruff, D. P. A Photoelectron Diffraction Investigation of Vanadyl Phthalocyanine on Au(1 1 1). *Surf. Sci.* **2010**, *604*, 47–53.

- (23) Baran, J. D.; Larsson, J. A. Structure and Energetics of Shuttlecock-Shaped Tin-Phthalocyanine on Ag(111): A Density Functional Study Employing Dispersion Correction. *J. Phys. Chem. C* **2012**, *116*, 9487–9497.

- (24) Niu, T.; Zhou, M.; Zhang, J.; Feng, Y.; Chen, W. Dipole Orientation Dependent Symmetry Reduction of Chloroaluminum Phthalocyanine on Cu(111). *J. Phys. Chem. C* **2013**, *117*, 1013–1019.

- (25) Kresse, G.; Furthmüller, J. Efficient Iterative Schemes for Ab Initio Total-Energy Calculations Using a Plane-Wave Basis Set. *Phys. Rev. B: Condens. Matter Mater. Phys.* **1996**, *54*, 11169–11186.
- (26) Perdew, J. P.; Burke, K.; Ernzerhof, M. Generalized Gradient Approximation Made Simple. *Phys. Rev. Lett.* **1996**, *77*, 3865–3868.
- (27) Perdew, J. P.; Burke, K.; Ernzerhof, M. Generalized Gradient Approximation Made Simple [Phys. Rev. Lett. 77, 3865 (1996)]. *Phys. Rev. Lett.* **1997**, *78*, 1396–1396.
- (28) Blöchl, P. E. Projector Augmented-Wave Method. *Phys. Rev. B: Condens. Matter Mater. Phys.* **1994**, *50*, 17953–17979.
- (29) Kresse, G.; Joubert, D. From Ultrasoft Pseudopotentials to the Projector Augmented-Wave Method. *Phys. Rev. B: Condens. Matter Mater. Phys.* **1999**, *59*, 1758–1775.
- (30) Marom, N.; Hod, O.; Scuseria, G. E.; Kronik, L. Electronic Structure of Copper Phthalocyanine: A Comparative Density Functional Theory Study. *J. Chem. Phys.* **2008**, *128*, 164107.
- (31) Marom, N.; Kronik, L. Density Functional Theory of Transition Metal Phthalocyanines, I: Electronic Structure of NiPc and CoPc—self-Interaction Effects. *Appl. Phys. A: Mater. Sci. Process.* **2009**, *95*, 159–163.
- (32) Huang, Y. L.; Wruss, E.; Egger, D. A.; Kera, S.; Ueno, N.; Saidi, W. A.; Bucko, T.; Wee, A. T. S.; Zojer, E. Understanding the Adsorption of CuPc and ZnPc on Noble Metal Surfaces by Combining Quantum-Mechanical Modelling and Photoelectron Spectroscopy. *Molecules* **2014**, *19*, 2969–2992.
- (33) Lüftner, D.; Milko, M.; Huppmann, S.; Scholz, M.; Ngyuen, N.; Wießner, M.; Schöll, A.; Reinert, F.; Puschnig, P. CuPc/Au(1 1 0): Determination of the Azimuthal Alignment by a Combination of Angle-Resolved Photoemission and Density Functional Theory. *J. Electron Spectrosc. Relat. Phenom.* **2014**, *195*, 293–300.
- (34) Hofmann, O. T.; Atalla, V.; Moll, N.; Rinke, P.; Scheffler, M. Interface Dipoles of Organic Molecules on Ag(111) in Hybrid Density-Functional Theory. *New J. Phys.* **2013**, *15*, 123028.
- (35) Lifshitz, E. M. The Theory of Molecular Attractive Forces between Solids. *Sov. Phys. JETP* **1956**, *2*, 73–83.
- (36) Zaremba, E.; Kohn, W. van der Waals Interaction between an Atom and a Solid Surface. *Phys. Rev. B* **1976**, *13*, 2270–2285.
- (37) Methfessel, M.; Paxton, A. T. High-Precision Sampling for Brillouin-Zone Integration in Metals. *Phys. Rev. B: Condens. Matter Mater. Phys.* **1989**, *40*, 3616–3621.
- (38) Monkhorst, H. J.; Pack, J. D. Special Points for Brillouin-Zone Integrations. *Phys. Rev. B* **1976**, *13*, 5188–5192.
- (39) Neugebauer, J.; Scheffler, M. Adsorbate-Substrate and Adsorbate-Adsorbate Interactions of Na and K Adlayers on Al(111). *Phys. Rev. B: Condens. Matter Mater. Phys.* **1992**, *46*, 16067–16080.
- (40) Bučko, T.; Hafner, J.; Ángyán, J. G. Geometry Optimization of Periodic Systems Using Internal Coordinates. *J. Chem. Phys.* **2005**, *122*, 124508.
- (41) Müllegger, S.; Schöffberger, W.; Rashidi, M.; Lengauer, T.; Klappenberger, F.; Diller, K.; Kara, K.; Barth, J. V.; Rauls, E.; Schmidt, W. G.; et al. Preserving Charge and Oxidation State of Au(III) Ions in an Agent-Functionalized Nanocrystal Model System. *ACS Nano* **2011**, *5*, 6480–6486.
- (42) Heinrich, B. W.; Ahmadi, G.; Müller, V. L.; Braun, L.; Pascual, J. I.; Franke, K. J. Change of the Magnetic Coupling of a Metal–Organic Complex with the Substrate by a Stepwise Ligand Reaction. *Nano Lett.* **2013**, *13*, 4840–4843.
- (43) Gutzler, R.; Walch, H.; Eder, G.; Kloft, S.; Heckl, W. M.; Lackinger, M. Surface Mediated Synthesis of 2D Covalent Organic Frameworks: 1,3,5-tris(4-Bromophenyl)benzene on graphite(001), Cu(111), and Ag(110). *Chem. Commun.* **2009**, No. 29, 4456.
- (44) Koch, M.; Gille, M.; Viertel, A.; Hecht, S.; Grill, L. Substrate-Controlled Linking of Molecular Building Blocks: Au(111) vs. Cu(111). *Surf. Sci.* **2014**, *627*, 70–74.
- (45) Crapper, M. D.; Riley, C. E.; Sweeney, P. J. J.; McConville, C. F.; Woodruff, D. P.; Jones, R. G. Investigation of the Cu(111) ( $\sqrt{3} \times \sqrt{3}$ )R30°-Cl Structure Using Sexafs and Photoelectron Diffraction. *Surf. Sci.* **1987**, *182*, 213–230.
- (46) Guilleme, J.; Martínez-Fernández, L.; González-Rodríguez, D.; Corral, I.; Yáñez, M.; Torres, T. An Insight into the Mechanism of the Axial Ligand Exchange Reaction in Boron Subphthalocyanine Macrocycles. *J. Am. Chem. Soc.* **2014**, *136*, 14289–14298.
- (47) De Renzi, V.; Rousseau, R.; Marchetto, D.; Biagi, R.; Scandolo, S.; del Pennino, U. Metal Work-Function Changes Induced by Organic Adsorbates: A Combined Experimental and Theoretical Study. *Phys. Rev. Lett.* **2005**, *95*, 046804.
- (48) Rusu, P. C.; Brocks, G. Work Functions of Self-Assembled Monolayers on Metal Surfaces by First-Principles Calculations. *Phys. Rev. B: Condens. Matter Mater. Phys.* **2006**, *74*, 073414.
- (49) Hill, I. G.; Rajagopal, A.; Kahn, A.; Hu, Y. Molecular Level Alignment at Organic Semiconductor-Metal Interfaces. *Appl. Phys. Lett.* **1998**, *73*, 662–664.
- (50) Crispin, X.; Geskin, V.; Crispin, A.; Cornil, J.; Lazzaroni, R.; Salaneck, W. R.; Brédas, J.-L. Characterization of the Interface Dipole at Organic/ Metal Interfaces. *J. Am. Chem. Soc.* **2002**, *124*, 8131–8141.
- (51) Crispin, A.; Crispin, X.; Fahlman, M.; Berggren, M.; Salaneck, W. R. Transition between Energy Level Alignment Regimes at a Low Band Gap Polymer-Electrode Interfaces. *Appl. Phys. Lett.* **2006**, *89*, 213503.
- (52) Koch, N. Organic Electronic Devices and Their Functional Interfaces. *ChemPhysChem* **2007**, *8*, 1438–1455.
- (53) Braun, S.; Salaneck, W. R.; Fahlman, M. Energy-Level Alignment at Organic/Metal and Organic/Organic Interfaces. *Adv. Mater.* **2009**, *21*, 1450–1472.
- (54) Hofmann, O. T.; Egger, D. A.; Zojer, E. Work-Function Modification beyond Pinning: When Do Molecular Dipoles Count? *Nano Lett.* **2010**, *10*, 4369–4374.
- (55) Edlbauer, H.; Zojer, E.; Hofmann, O. T. Postadsorption Work Function Tuning via Hydrogen Pressure Control. *J. Phys. Chem. C* **2015**, *119*, 27162–27172.